Design and Analysis of Robust Minimax LQG Controller for an Experimental Beam Considering Spill-Over Effect

Allahyar Montazeri, Javad Poshtan, and Aghil Yousefi-Koma

***Abstract*—In this brief the design and analysis of an optimal robust minimax linear quadratic Gaussian (LQG) control of vibration of a flexible beam is studied. The analysis is performed by transforming the minimax LQG control design problem to its equivalent mixed sensitivity design problem. The first six modes of the beam in the frequency range of 0–700 Hz are selected for control purpose. Among these modes, three modes in the frequency range of 100–400 Hz are used for control, while the other three modes are left as the uncertainty of modeling. Both the model and the uncertainty are measured based on experimental data. The nominal model is identified from frequency response data and the uncertainty is presented by frequency weighted multiplicative modeling method. For the augmented plant consisting of the nominal model and its accompanied uncertainty, a minimax LQG controller is designed. Analysis and tradeoff between robust stability and robust performance is shown by selecting two different choices of uncertainty modeling. Simulation results used to show how the uncertainty weights can be tuned so that the proposed robust controller increase the damping of the system in its resonance frequencies and maintain the robust stability of the feedback system at the same time.**

***Index Terms*—Active vibration control, minimax linear quadratic Gaussian (LQG) control, robust performance, robust stability.**

I. Introduction

NOISE and vibration have caused many problems for most of industries and these are growing in recent years. For example the new generations of in ground, aerial, and space vehicles are made from advanced and light weight structures due to economical and environmental reasons. This in turn, will cause the increasing amount of vibration and the noise emitted from vehicles and their structures as well. Passive methods (using isolators, adding extra mass,...) are not suitable in low-frequency noise and vibration applications, because they increase the volume and the weight of structures and are unable to adapt with environmental changes. An interesting alternative solution which has been the main subject of many researches in recent years is to actively control noise and vibrations especially by the use of smart materials [1], [2]. In fact, progress in the field of smart structures and material systems as well as in microelectronics science [especially evolution of the fast digital signal processing (DSP) processors] has increased interest in the use of active noise and vibration control (ANVC) systems as a solution of related industrial problems. For applications in aerospace and automobile industries, interested readers can refer to [3] and [4]. Classical controllers which are frequently used in collocated arrangements are suitable, especially when it is possible to control each mode separately based on the local information of that mode [5], [6]. Such controllers are usually decentralized, and their stability and also stability robustness conditions are not known in general.

The use of robust controllers for active suppression of noise and vibrations has been studied and developed in recent years [7]–[9]. Spatially robust H_2 and H_∞ controllers for control of vibrations in an experimental beam are designed and tested in [10] and [11]. To eliminate vibration on the entire beam, an appropriate cost functional indicating the vibration energy of the structure is selected, and an optimal controller considering limits on the actuator signals is designed. The use of H_∞ norm in the design of robust controllers will lead to a conservative control system and the performance of such controllers is usually not satisfactory. To alleviate this problem, and obtain a controller with robust performance and robust stability properties, μ-synthesis technique has been introduced. The use of μ-synthesis in robust control of vibration in flexible structures was investigated by [12] and [13]. A more suitable criterion for minimization is to use H_2 norm of performance index. However, design of robust H_2 controllers is computationally intractable, and there is no analytic solution for them [14]. Since LQG controllers are special cases of H_2 controllers for Gaussian signals, considering robustness issues in linear quadratic Gaussian (LQG) controllers will result in a controller with good nominal and robust performance. A minimax LQG controller in which the worst-case LQG performance index is minimized is such a controller [15]. The use of minimax LQG control in active vibration control applications has been reported in [16]. This controller is designed in worst case and can withstand two kinds of uncertainties: structured and unstructured modeling uncertainties as well as unpredictable disturbances acting on the system. Unlike H_2 and H_∞ controllers in which a non-convex performance index is optimized, the minimax LQG controller is obtained by minimizing a convex optimization problem and solving two steady-state H_∞-type algebraic Riccati equations [15].

In this brief, an approach close to [16] is adopted for controller design; however, the plant selected for design and analysis is quite different. Particularly, in this study, modes two, three, and four of a flexible beam with clamped boundary conditions are considered for control purpose, and the other three modes in the control bandwidth are left as uncertainty. Besides, the model considered for control is non-minimum phase with

Manuscript received September 03, 2008; revised May 10, 2009 and March 31, 2010; accepted April 24, 2010. Manuscript received in final form August 24, 2010. Recommended by Associate Editor M. Mesbahi.

A. Montazeri and J. Poshtan are with the Faculty of Electrical Engineering, Iran University of Science and Technology, Narmak 16846, Tehran, Iran (e-mail: amontazeri@iust.ac.ir; jposhtan@iust.ac.ir).

A. Yousefi-Koma is with the Faculty of Mechanical Engineering, College of Engineering, University of Tehran, Tehran 16846, Iran (e-mail: aykoma@ut.ac.ir).

Digital Object Identifier 10.1109/TCST.2010.2071873

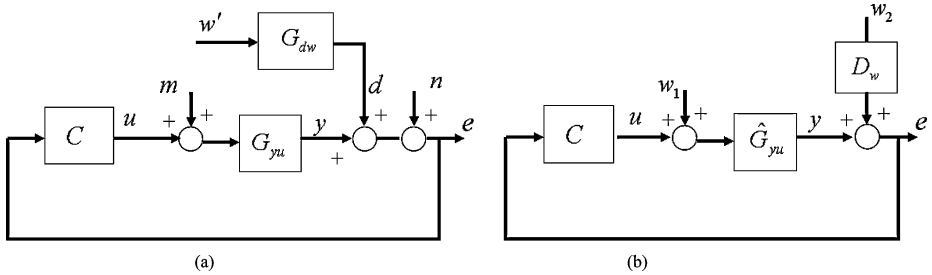

Fig. 1. (a) Block diagram of a feedback active control problem. (b) Nominal feedback active control system after removing the effect of primary disturbance.

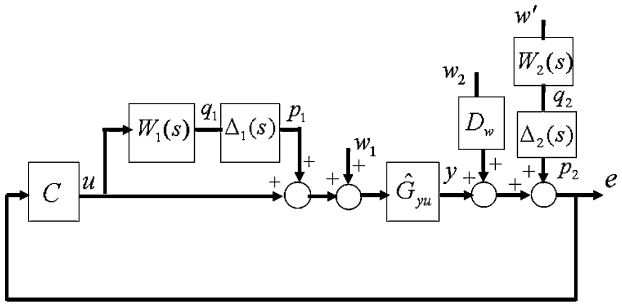

Fig. 2. Block diagram of feedback active control system including uncertainties.

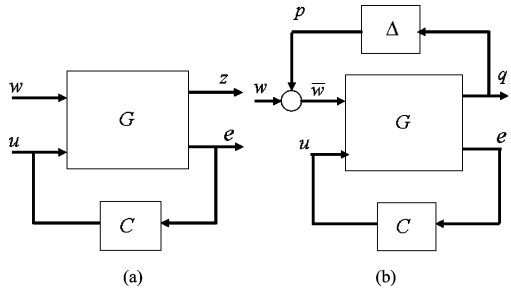

Fig. 3. (a) LFT representation of the nominal active control system shown in Fig. 1(b). (b) LFT representation of the perturbed active control system shown in Fig. 2.

two complex conjugate zeros in the right-half of the s-plane which in turn, due to waterbed effect, will make the feedback control problem much more difficult. This type of model is the case in many active noise and vibration control problems especially when we are interested to control modes in a specific bandwidth. Moreover, the amplitude of the uncertainties considered in this study, in contrast to [16], has large amplitude at low and high frequencies. In fact, because of lightly damped nature of the resonant frequencies in active noise and vibration control systems, this type of uncertainty is common when a part of the dynamics of the system is neglected or uncertainty is generated due to the movement of resonant frequencies resulting from aging or temperature changes. For this purpose, in Section II a linear fractional transformation (LFT) form of the feedback active control problem with uncertainties in primary and secondary paths is derived, and the minimax LQG control problem is formulated and solved based on it. Since the focus of the current study is to reveal how one can achieve a compromise between robust stability and robust performance in the design of the minimax LQG controller, in Section III two kinds of weighting functions are selected for uncertain system model. The obtained results are explained in Section IV more intuitively by considering an equivalent H_∞ control problem corresponding to the minimax LQG problem. This will allow us to represent the minimax LQG control problem with a four-block H_∞ control problem, in which the effect of different design parameters for robust stability and performance tradeoff can be viewed more clearly.

II. Problem Formulations

A. Nominal Control System Architecture

A typical block diagram of a feedback active control system is shown in Fig. 1(a). In this figure, G_{dw} and G_{yu} represent the actual primary and secondary path transfer functions, respectively, and C is the controller transfer function. Although in most cases just an estimation of primary and secondary paths is available, for simplicity it is first assumed these transfer functions are exactly the same as the real transfer function. In this case, by subtracting the effect of the disturbance passing through the primary path the block diagram of the feedback active control system can be simplified as shown in Fig. 1(b). In this figure, $\hat{G}_{yu}$ is an estimation of G_{yu} and D_w is a gain used to tune the effect of measurement noise at the output of the plant. By representing the block diagram of Fig. 1(b) with its equivalent LFT form in Fig. 3(a), the inputs, outputs, and generalized plant G will be defined by

$$G=\left[\begin{array}{cc|c} \hat{G}_{yu} & D_w & \hat{G}_{yu} \\ 0 & 0 & R^{\frac{1}{2}} \\ \hline \hat{G}_{yu} & D_w & \hat{G}_{yu} \end{array}\right], \quad w=\begin{bmatrix} w_1 \\ w_2 \end{bmatrix}, \quad z=\begin{bmatrix} e \\ R^{\frac{1}{2}}u \end{bmatrix}. \tag{1}$$

In (1), w is the vector of input noises, z is the predefined performance measure, and R is the weighting parameter used to penalize the control effort. If one knows the state-space realization of the secondary path, the state space realization of the generalized plant of nominal system can be written as

$$\begin{aligned} \dot{x}_m &= Ax_m + B_1 w_1 + B_2 u \\ z &= C_1 x_m + D_{11} w_1 + D_{12} u \\ e &= C_2 x_m + D_{21} w_2 + D_{22} u \end{aligned} \tag{2}$$

where

$$\hat{G}_{yu} = \begin{bmatrix} A_m & B_m \\ C_m & D_m \end{bmatrix}$$

$$A = A_m, B_1 = B_m, B_2 = B_m$$

$$C_1 = \begin{bmatrix} C_m \\ 0 \end{bmatrix}, \quad D_{11} = \begin{bmatrix} 0 \\ 0 \end{bmatrix}, \quad D_{12} = \begin{bmatrix} 0 \\ R^{(1/2)} \end{bmatrix}$$

$C_2 = C_m, \quad D_{21} = D_w, \quad D_{22} = D_m = 0$. Here w_1 and w_2 are white Gaussian noises with zero mean and unit covariance, and the signal z is used to evaluate the performance of the closed-loop control system.

The classical feedback controller which is able to reduce disturbance and noise at the output of the control system is designed using LQG theory. This controller will be calculated by setting $D_{11} = \begin{bmatrix} 0 \\ 0 \end{bmatrix}$ in (2), and minimizing the performance index J

$$J = \lim \quad \frac{1}{T} \; E \; \int_0^T z(t)^T z(t) \; dt \qquad T \to \infty. \tag{3}$$

B. Perturbed Control System Architecture

Since in most practical ANVC systems uncertainties occur during the normal operation of the system it is necessary to design a controller that exhibits robustness properties against these kinds of uncertainties. One of the sources of uncertainties in active control systems is neglecting part of the dynamics of the system under control. Fundamentally, lightly damped mechanical or acoustical systems are distributed-parameter systems, and thus have infinite dimensional analytic models. In order to design a finite dimensional (preferably low-order) controller, one has to have a finite dimensional model of the dynamical system in the interested frequency range of the controller. By using truncated or reduced-order models, "spillover effect" is a possible phenomenon. Generally, spillover effect is considered as the degradation of controller performance due to excitation of unmodeled dynamics. However, by a more general definition by [17], this is unavoidable even if the system model is a completely accurate representation of the physical system. In fact spillover will happen in a feedback active control system if either of the secondary and disturbance sources or the performance and measurement sensors are collocated [17]. This is exactly the case in our minimax LQG controller design in Fig. 2, in which it is assumed that the disturbance and control signals are entered through the same channel. This necessitates taking into account the unmodelled dynamics (or generally the frequency range which is not the target of the controller) by exploiting suitable weighting functions in a robust controller design framework.

A method commonly used to capture the uncertainties exist in the model of a systems in a control application is multiplicative uncertain system modeling. In fact if there are some degrees of uncertainty in the model of secondary and primary paths in the feedback active control system and they can be modeled as multiplicative uncertainty at the input of the plant, the block diagram of Fig. 1(a) can be modified to the block diagram shown in Fig. 2. In this figure, W_1 and W_2 are two weighting functions used to normalize the uncertainties in the secondary and primary paths so that $\|\Delta_i\|_\infty \leq 1$ for $i = 1, 2$. Since w', and w_2 are white Gaussian noises with zero mean and unit covariance they can be assumed the same in the modeling. By transforming the block diagram of Fig. 2 to the generalized form, it can be represented in the LFT form suitable for design of minimax LQG controller as mentioned in [16] and [18].

The inputs, outputs and generalized plant G will be defined by

$$G = \left[\begin{array}{cc|c} 0 & 0 & W_1 \\ 0 & W_2 & 0 \\ \hline \hat{G}_{yu} & D_w & \hat{G}_{yu} \end{array}\right], \quad \bar{w} = \begin{bmatrix} \bar{w}_1 \\ \bar{w}_2 \end{bmatrix}, \quad q = \begin{bmatrix} q_1 \\ q_2 \end{bmatrix}. \tag{4}$$

The inputs and outputs of uncertainty block are denoted by $q = \begin{bmatrix} q_1 \\ q_2 \end{bmatrix}$ and $p = \begin{bmatrix} p_1 \\ p_2 \end{bmatrix}$ in Fig. 3(b) and are related by a diagonal uncertain matrix

$$\Delta = \begin{bmatrix} \Delta_1 & 0 \\ 0 & \Delta_2 \end{bmatrix} \tag{5}$$

where it is assumed that both Δ_1 and Δ_2 have infinity norm less that one. In fact the signals p_1 and p_2 which are the outputs of uncertainty in the primary and secondary paths can be viewed as the cause of perturbation in the nominal excitation signal shown in Fig. 3(a). This LFT representation is a more convenient form in the design of robust controller which will be described in Section IV. It must be noted that because of simplicity and without loss of generality in the next sections it is assumed that the uncertainty exists just in the model of the secondary path and the effect of disturbance passing through the primary path is completely removed.

III. Experimental Setup and Model of the Beam

A. Nominal Plant Identification

The flexible structure considered for this study is an aluminum beam with clamped boundary conditions. The experimental setup and different parts used for data acquisition and measurement of the frequency response function (FRF) of the beam in the frequency range of 0–700 Hz are shown in Figs. 4 and 5. This measured FRF, shown in Fig. 6, works as the basis for the identification of the nominal model of the secondary path and its accompanied uncertainty. The frequency range of 0–700 Hz which contains the first six modes of the beam is considered as the interested bandwidth. Here the concentrate is to design a feedback controller which is robust against spillover effect. To be able to consider the effect of spillover as a result of truncation or model reduction, approximately half of the bandwidth in the frequency range of 0–340 Hz is selected for control purpose. Generally, fitting a transfer function by using only experimental frequency response data might produce poor matching or even unstable system with respect to the time-domain response of the beam [19]. Moreover, it should be noted that increasing the order of the transfer function to have a better fit to the measured FRF may also cause numerical problems. Considering these facts, and also to extend the work carried out in [16] to a more general plant with lower order model of the beam, a six-order transfer function with reasonable fit to the measured FRF in the selected bandwidth has been designed. In fact, because of the low order denominator of this transfer function, it is only possible to model the second, third, and fourth modes of the beam. Hence, the fifth and sixth modes of the beam are considered as the uncertainty come up due to the truncation of the high order dynamics of the beam, and the

Fig. 4. Experimental setup used for measuring the FRF of the beam.

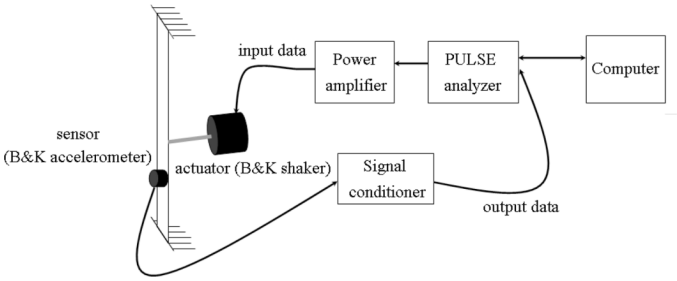

Fig. 5. Path of input and output signals used for data acquisition.

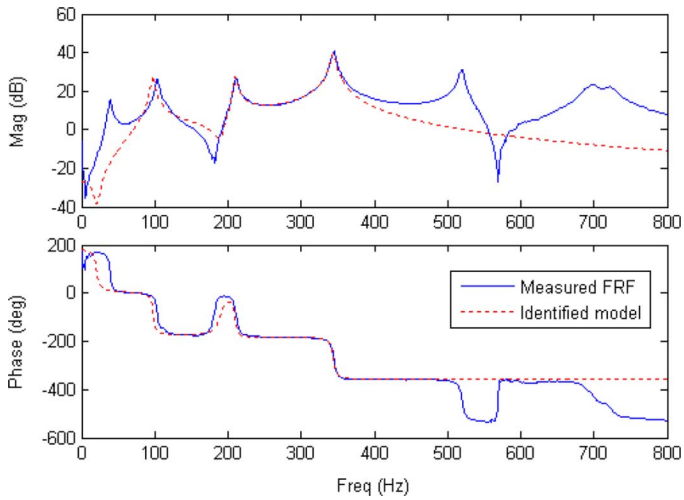

Fig. 6. Measured (solid line) and identified (dashed line) frequency response of the beam.

first mode of the beam is regarded as the uncertainty related to the low order transfer function selected for its model. In this way the bandwidth interested for control is the frequency range of 100–400 Hz, and the out-bandwidth modes may degrade the performance or even cause instability because of spillover effect. Fig. 6 shows the magnitude and phase of the measured FRF and the transfer function fitted to it. The degree of numerator and denominator of the identified model are chosen 4 and 6, respectively. This is in agreement with the analytical model of the beam from which a second order transfer function is dedicated to each mode. The transfer function of the fitted model is shown in (6) at the bottom of the page.

To make sure that the identified model matches also in time domain and is reliable for designing a controller that compensates the time-domain response of the beam despite the frequency response, the impulse responses of the measured and identified model of the beam are plotted in Fig. 7. These impulse responses are calculated by taking the inverse FFT of the measured and identified FRF, and selecting a suitable sampling frequency with respect to the interested bandwidth of the system. These results show that the transfer function $\hat{G}_{yu}$ which is identified based on the frequency domain data could capture the time domain response of the flexible beam, and hence is suitable for design of the robust controller to modify both time and frequency responses of the beam. It should be noted that we do not intend to compare these two impulse responses exactly because they belong to two different systems. However, it is important to notice that they show rather the same behavior in the sense that a subset of modes that contribute to the impulse response of G_{yu} are used in the impulse response of its estimate $\hat{G}_{yu}$.

B. Uncertainty Modeling

In the design of minimax LQG controller not only having a nominal model of the flexible structure in the desired frequency band is necessary, but also the class of uncertainty for which the controller is designed should be specified. The identified transfer function (6) is chosen as the nominal model of the beam. This model is used for the controller design and performance

$$\hat{G}_{yu}(s) = \frac{-2.555s^4 - 0.0615s^3 - 1.628s^2 + 0.00352s - 0.01232}{s^6 + 0.056s^5 + 3.013s^4 + 0.106s^3 + 2.077s^2 + 0.0350s + 0.267}. \quad (6)$$

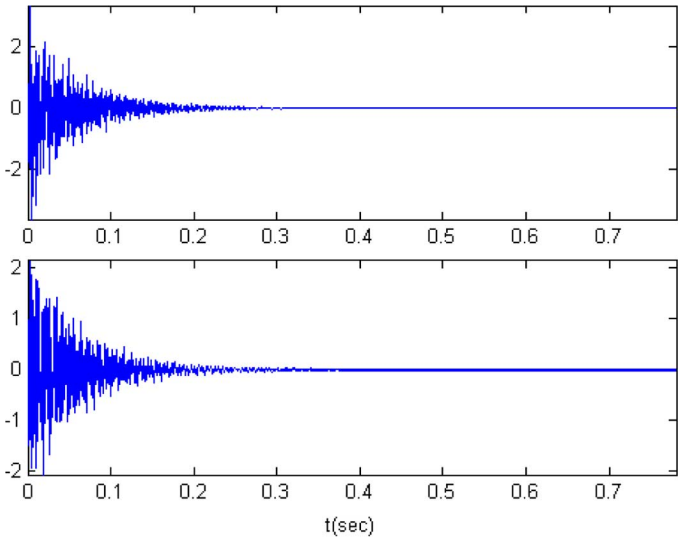

Fig. 7. Impulse responses of the measured (top) and identified (bottom) model of the beam corresponding to frequency response data of Fig. 6.

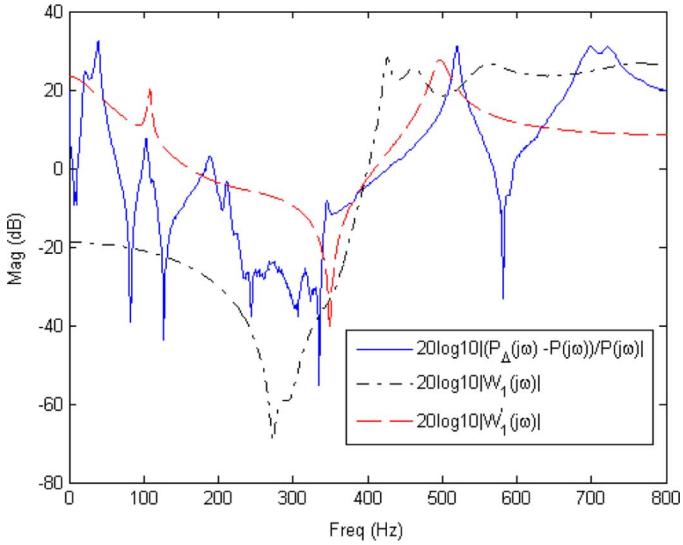

Fig. 8. Magnitude of uncertainty (solid line), multiplicative uncertain bound for Chebychev filter (dashed-dotted line), multiplicative uncertain bound for Pth norm filter (dashed line).

evaluation in the rest of this brief. By considering the uncertainty of this nominal model as a multiplicative uncertainty, the real model of the beam, considering Fig. 2, can be written as

$$G_{yu}(s) = \hat{G}_{yu}(s)(1 + W_1(s)\Delta_1(s)). \tag{7}$$

Here $W_1(s)$ is the weighting function used to normalize the uncertainty in different frequencies. The normalized uncertainty $\Delta_1(s)$ is assumed to satisfy the following condition:

$$\| \Delta_1(s) \|_\infty \leq 1. \tag{8}$$

A smaller norm will increase the stability margin but the performance may be decreased. To guarantee the inequality in (8), the weighting function $W_1(s)$ must be calculated such that the following inequality holds:

$$|W_1(j\omega)| \geq \left| \frac{G_{yu}(j\omega) - \hat{G}_{yu}(j\omega)}{\hat{G}_{yu}(j\omega)} \right|. \tag{9}$$

To achieve a good tradeoff between stability robustness and performance of the controller, this part of design procedure is crucial in a robust controller design. The weighting function $W_1(s)$ in the multiplicative uncertainty of the plant is modeled with two filters as shown in Fig. 8. The first one is a Chebychev type-I filter of order 11, and the second one is chosen a Pth-norm filter. The first filter is achieved by subtracting bode plots of two high-pass analog filters with different cutoff frequencies so that the poles of the filter with lower cutoff frequency will be the zeros of the new filter, and the fall off in the middle frequencies of the Chebychev filter in Fig. 8 corresponds to the frequency of these zeros. Since the main effect of the weighting filter here is to shape the loop gain of the feedback control system, proper tuning of its magnitude at different frequencies plays an important role on achieving a suitable robust performance and stability tradeoff in design of the controller. For that reason, the characteristics of both weighting filters such as cut off frequency, order, and pass-band ripples has to be adjusted carefully after some trials and errors. This is done by using the FDA toolbox of MATLAB and then designed digital filter is converted to an analog filter by using Tustin method. The resulted analog filter will set an upper bound on the uncertainties of the model of the system. As it is clear from Fig. 8, for Chebychev filter the fit is not tight to the unmodeled dynamics. In fact, by violating the inequality of (9) a less conservative controller will be designed. It will be shown in Section IV that in design of minimax LQG controller we can do this by a scaling factor and still retain the sufficient condition for the robust stability of the control system. However, as simulation results will also confirm, by compromising between this loose/tight fitting a better tradeoff between robust performance and robust stability of the closed-loop system will be achieved. It must be noted that although increasing the order of the weighting filter will result in a better fitting, it will increase the order of the model and hence the designed controller. This in turn may cause numerical instability in the design of the controller and make it unstable.

IV. Robustness Analysis of Minimax LQG Controller

In this section the robustness analysis of the minimax LQG controller is presented. A complete and rigorous description of the minimax LQG control theory can be found in [15] and [18]. By writing the state-space realization of the estimated model of the secondary path as well as its associated weighting function the state-space realization of the open-loop generalized plant G in Fig. 3(b), when the uncertainty exists just in the model of the secondary path can be written as

$$\begin{aligned} \dot{\bar{x}} &= \bar{A}\bar{x} + \bar{B}_1\bar{w}_1 + \bar{B}_2 u \\ q_1 &= \bar{C}_1\bar{x} + \bar{D}_{11}\bar{w}_1 + \bar{D}_{12}u \\ e &= \bar{C}_2\bar{x} + \bar{D}_{21}w_2 + \bar{D}_{22}u \end{aligned} \tag{10}$$

where $\bar{x} = [x_m \quad x_u]^T$

$$\hat{G}_{yu} = \begin{bmatrix} A_m & B_m \\ C_m & D_m \end{bmatrix}, \quad W_1 = \begin{bmatrix} A_u & B_u \\ C_u & D_u \end{bmatrix},$$

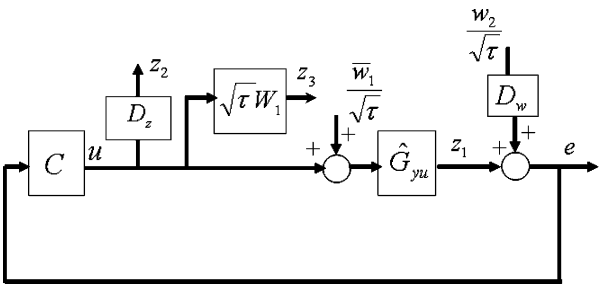

Fig. 9. Equivalent diagram of H_∞ representation of the minimax LQG control problem.

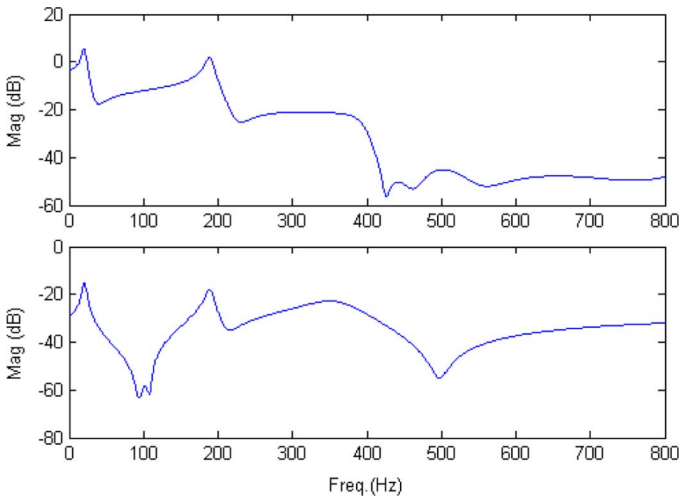

Fig. 10. (Top) Controller magnitude bode plot for Chebychev uncertainty weighting. (Bottom) Controller magnitude bode plot for Pth-norm uncertainty weighting.

$$\bar{A} = \begin{bmatrix} A_m & 0 \\ 0 & A_u \end{bmatrix}, \quad \bar{B}_1 = \begin{bmatrix} B_m \\ 0 \end{bmatrix}, \quad \bar{B}_2 = \begin{bmatrix} B_m \\ B_u \end{bmatrix}$$

$\bar{C}_1 = [0 \;\; C_u]$, $\bar{D}_{11} = 0$, $\bar{D}_{12} = D_u$, $\bar{C}_2 = [C_m \;\; 0]$, $\bar{D}_{21} = D_w$, $\bar{D}_{22} = 0$.

Besides, the relation between the input and output of the uncertainty model may be written in the general integral quadratic constraint (IQC) form as follows:

$$\lim \quad \frac{1}{T} E\left[\int_0^T ||p_1(t)||^2 \, dt - \int_0^T ||q_1(t)||^2 \, dt\right] \leq d \quad T \to \infty \tag{11}$$

where d is a parameter that restricts the size of the total uncertain disturbance acting on the system. The performance of the minimax LQG active control system can be evaluated by adding this equation to (10)

$$z = \begin{bmatrix} C_z \\ 0 \end{bmatrix} \bar{x} + \begin{bmatrix} 0 \\ D_z \end{bmatrix} u. \tag{12}$$

In this case the performance index which must be minimized for the design of a minimax LQG controller is similar to the standard LQG problem in (3), unless there are some additional constraints on uncertainties defined by the IQC (11). In (12), C_z is the state weighting matrix and D_z is the weighting matrix on the input and limits the control effort. This weight is usually selected large enough to prevent the saturation of the control signal.

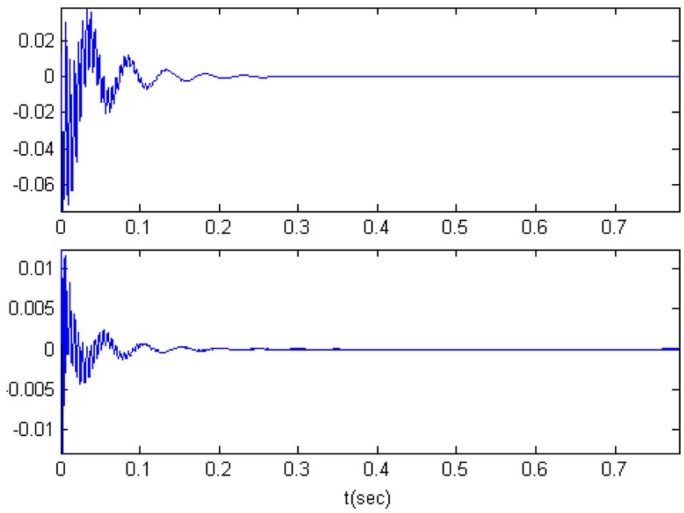

Fig. 11. (Top) Impulse response of the controller for Chebychev uncertainty weighting. (Bottom) Impulse response of the controller for Pth-norm uncertainty weighting.

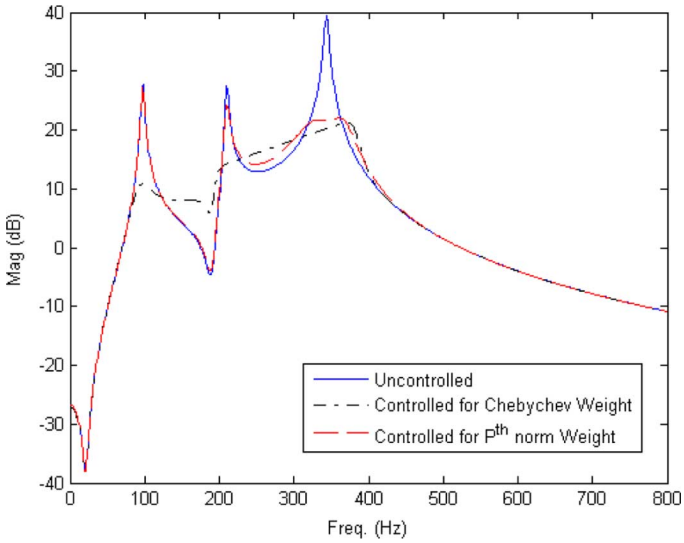

Fig. 12. Uncontrolled frequency response of the beam (solid line), Controlled frequency response of the beam with Chebychev uncertainty weighting (dashed-dotted line), Controlled frequency response of the beam with Pth norm uncertainty weighting (dashed line).

By combining the set of (10)–(12) with the performance index (3), it can be shown that the solution of the minimax LQG problem can be obtained by solving its equivalent standard H_∞ control problem. This is described by Theorem 1 as follows, however, due to lack of space the proof is omitted and an interested reader can refer to [15] and [18] for more theoretical details.

Theorem 1 [18]: The stabilizable solution of the H_∞ control problem defined by the system of equations

$$\dot{\bar{x}} = \bar{A}\bar{x} + \frac{\bar{B}_1}{\sqrt{\tau}}\bar{w}_1 + \bar{B}_2 u$$

$$z = \begin{bmatrix} C_z \\ 0 \\ \sqrt{\tau}\bar{C}_1 \end{bmatrix} \bar{x} + \begin{bmatrix} 0 \\ D_z \\ \sqrt{\tau}\bar{D}_{12} \end{bmatrix} u$$

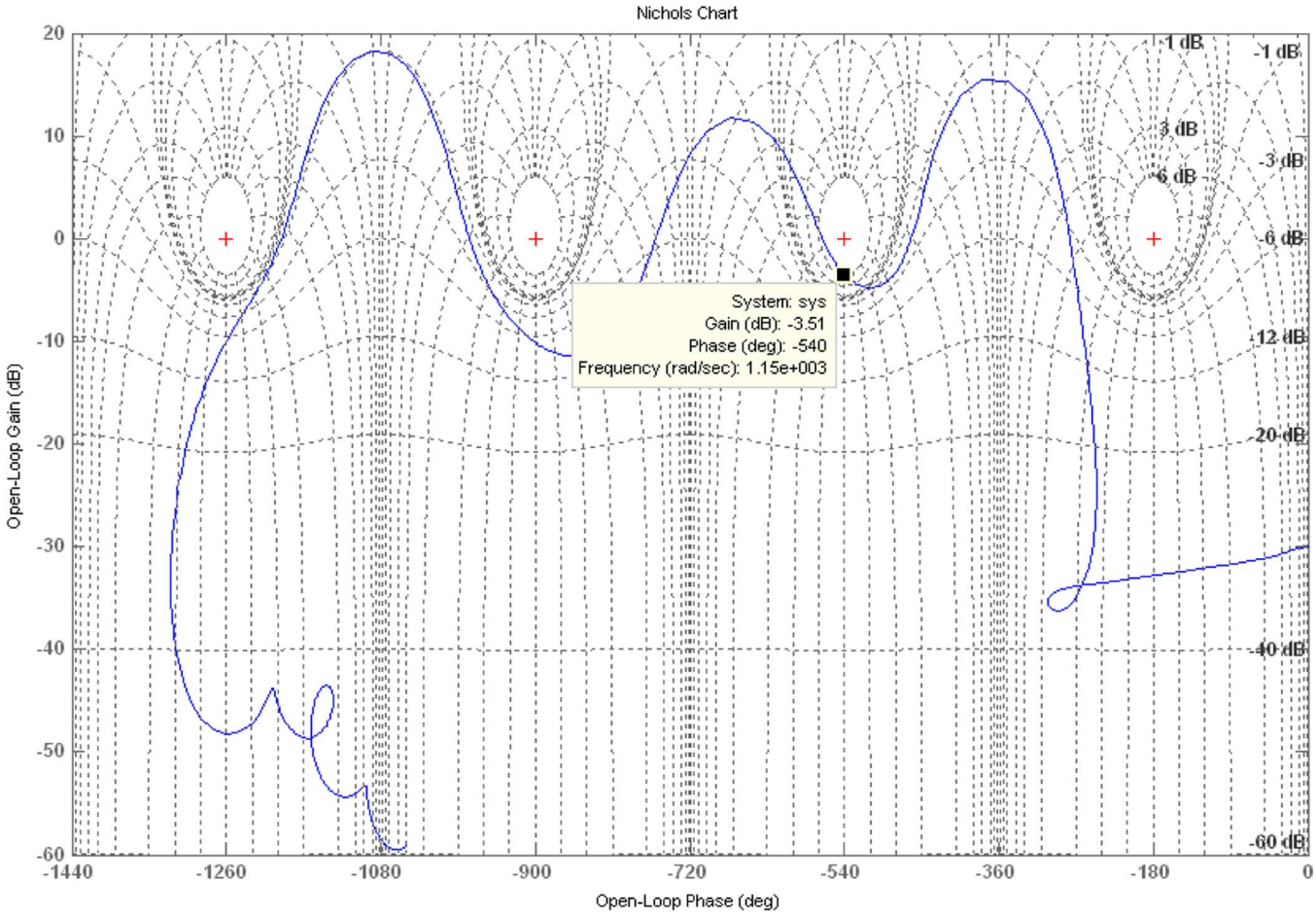

Fig. 13. Nichols chart of the loop gain to demonstrate stability margins of the closed-loop system for Chebychev uncertainty weighting.

$$e = \bar{C}_2 \bar{x} + \frac{\bar{D}_{21}}{\sqrt{\tau}} w_2 \tag{13}$$

and lead to the closed-loop transfer function from $\bar{w}_1$ to z with infinity norm less than one is exactly the same as the solution of the minimax LQG problem, defined by the system of (10), (12) and IQC (11) by which the performance index (3) is minimized. Here w_1 and w_2 are disturbance input and additive measurement noise respectively. By assuming C_z equal to $\bar{C}_2$ the first element of z, denoted by z_1 will be a measure of the error signal in Fig. 2. By transforming the minimax LQG problem to its equivalent H_∞ control problem, the performance and stability robustness of this controller can be analyzed more intuitively. This is obtained by drawing the block diagram representation of the state-space (13) as shown in Fig. 9. In fact by writing the transfer functions between different inputs and outputs of the plant, the H_∞ controller design can be casted into a so-called *four-block* H_∞ control problem [20].

Therefore, the problem of designing the minimax LQG controller is equivalent to find the controller C in Fig. 9 so that the following norm, which is trading off robust stability against performance, will be minimized:

$$\inf_{C\ stablz} \left\| \begin{matrix} \frac{1}{\sqrt{\tau}} S\hat{G}_{yu} & \frac{D_w}{\sqrt{\tau}} T \\ W_1 T & D_w W_1 C S \\ \frac{1}{\sqrt{\tau}} D_z T & \frac{1}{\sqrt{\tau}} D_z D_w C S \end{matrix} \right\|_\infty < 1 \tag{14}$$

where $S = (I + \hat{G}_{yu}C)^{-1}$ and $T = (I + \hat{G}_{yu}C)^{-1}\hat{G}_{yu}C$ are standard sensitivity and complementary sensitivity function, respectively. The minimization problem (14) shows the effect of different parameters including D_z, D_w, W_1, τ on the performance of the closed-loop control system. As a matter of fact, the uncertainty weight W_1, acts as a weighting function to shape the complementary sensitivity T which is important to assure the robust stability of the closed-loop system. Besides, high value of the parameter τ penalizes the disturbance rejection transfer functions of the closed-loop system in (14), and hence will force the optimizer to minimize the second row of (14), which results in better robust stability for the closed-loop system. As a result to have a better tradeoff between the performance and robust stability of the closed-loop system, the weighting function W_1 can be scaled with the parameter $1/\sqrt{\tau}$ to reduce its magnitude so that less conservatism is obtained in the design procedure.

V. Simulation/Experimental Results

In this section, the aim is to verify and compare the results of the designed minimax LQG controllers for the identified model in Section III, and its associated uncertainties. In fact the performances of the designed controllers are simulated using experimental data, and no explicit experimental implementation of the control system was attempted due to the lack of necessary actuators. However, the results are sufficient to demonstrate the difficulties which may occur in the design of a controller in real

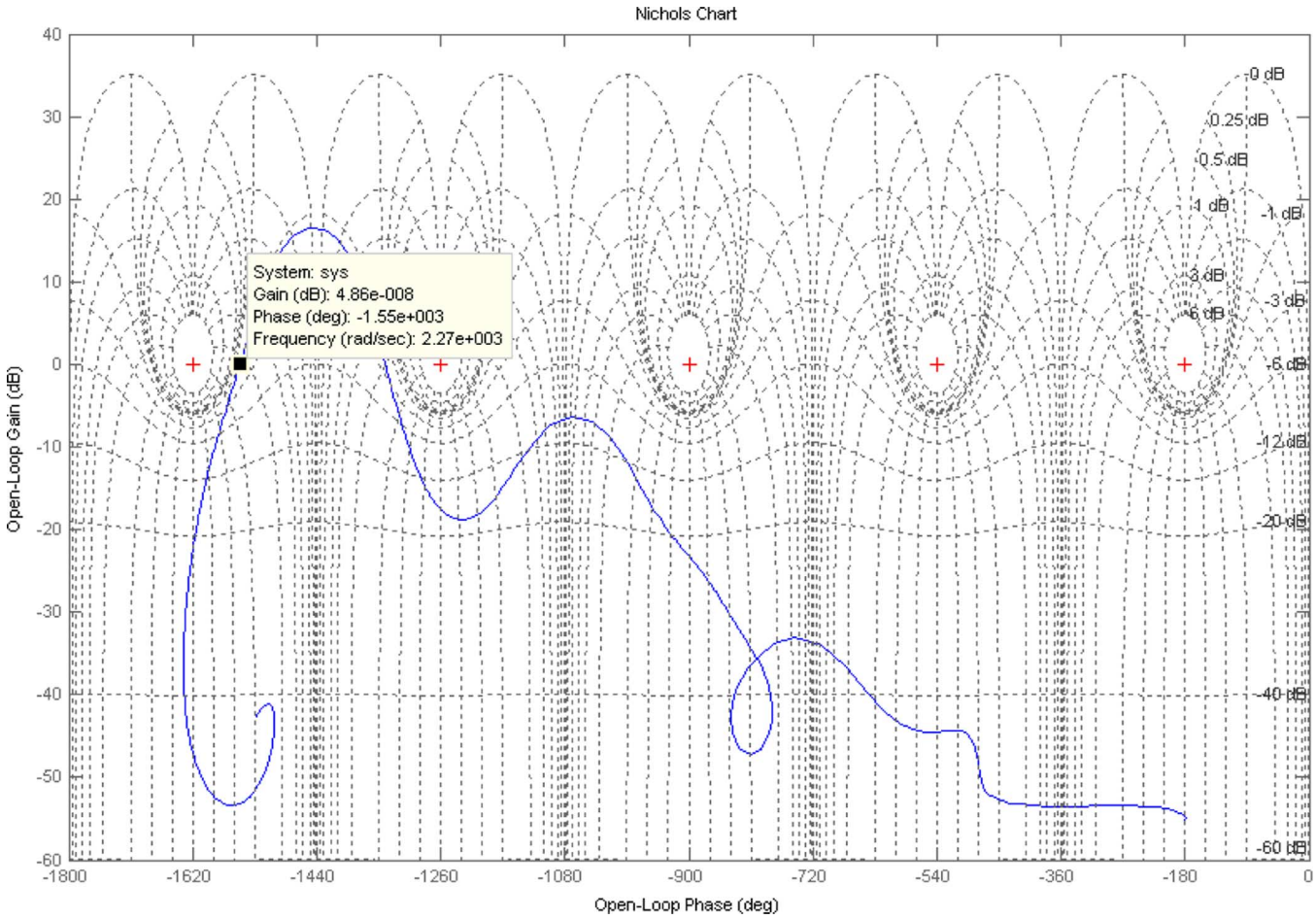

Fig. 14. Nichols chart of the loop gain to demonstrate stability margins of the closed-loop system for Pth-norm uncertainty weighting.

applications such as how the spillover will degrade the performance of the closed-loop system or even may cause instability.

As mentioned earlier, selecting a large d in (11) may result in good robust stability in the presence of uncertainties in the distribution of primary noise, but on the other hand it will deteriorate the performance of the closed-loop system. Besides, the increase of d can increase the cost functional linearly. Since here the aim is to consider just unmodeled high and low dynamic uncertainties, and not the uncertainties in the primary noise, d was chosen a small number equal to 10^{-10}. Selecting this small number will have the benefit that does not put extra weight on the uncertainties and reduce the conservatism of the designed controller. Since the complementary sensitivity and control effort are weighted in the second row of (14) by W_1, D_z is selected a small scalar equal to 10^{-4}. Indeed, by suitable tuning of the gain of W_1 it is possible to penalize the control effort and by setting a small value for D_z in the third row of (14) we can somehow compromise this effect to get a good result. The parameter D_w which shows the effect of measurement noise on the error signal has a great effect on the value of the cost functional and was chosen 10^{-3}. To find a solution for the minimax LQG problem formulated in Section II, the first step is to find the supremum of the quadratic cost (3) along with the set of uncertainties defined by (11) as the constraint. To convert the problem from a constrained optimization problem into an unconstraint optimization problem it is possible to use the method of Lagrange multipliers. Indeed, by defining the constant parameter τ as the multiplier of the augmented cost function it can be shown that maximizing this cost function will be equivalent to finding the infimum of a cost functional W_τ as a function of τ [18]. To find the value of τ for each type of uncertainties, the performance index W_τ for different values of τ is plotted. This helps to find the intervals where the global infimum of the cost functional may be found. Then with a more exact search using a nonlinear optimization algorithm, the fine tuning of τ was performed. It should be noted that a small change in τ may impair the performance of the system. By finding two different values of τ for the selected uncertainty models, the robust controller can be designed. The value of τ and its corresponding cost function for two uncertainty weights are

$$\begin{aligned} \tau_1 &= 197.2 \qquad W_{\tau_1} = 18\,883.77 \\ \tau_2 &= 931.6 \qquad W_{\tau_2} = 42\,026.41 \end{aligned} \tag{15}$$

where the first index is for Chebychev filter, and the second one is for Pth-norm filter.

The frequency responses of two designed controllers are plotted in Fig. 10. It can be inferred from this figure that the robust controller has the same nature as the plant, and the resonant peaks of the controllers occur near the resonant peaks of the plant. As stated earlier, the aim of these two controllers is to decrease the resonant peaks of the frequency response of the

beam, while holding the robust stability condition with respect to unmodelled dynamics. Open- and closed-loop frequency responses of the plant for two uncertainty weights are shown in Fig. 10. As can be seen in this figure, the damping of the modes for the first controller is greater than that of the second controller. This can be described as a result of a tighter uncertainty bound in the design of this controller. In fact, noting the discussion of previous section, the minimizing problem (14) reveals that the shape of the uncertainty weight has a determinant effect on the shape of the complementary sensitivity function. Explicitly speaking, at low and high frequencies of the Pth norm weighting function where its magnitude is large, the optimizer will force the magnitude of the complementary sensitivity and the control effort transfer functions of the closed-loop system to be low, and this is obtained by reducing the magnitude of the controller. This can be clearly seen by comparing the magnitude of the controllers in Fig. 10. On the other hand, reducing the loop gain as a result of the reduction of the control effort will deteriorate the disturbance rejection performance of the closed-loop control system. The bad performance of the controller for the first two modes in Fig. 12 (Pth norm filter) is the result of this phenomenon. Certainly this bad performance is traded off by large robust stability margins that may occur even in the controller bandwidth. The stability margins of both controllers at some frequencies near the critical point $(-1+j0)$ are shown in Figs. 13 and 14. The comparison of magnitude of both controllers with the magnitude of the FRF of the beam in Fig. 6, confirms that the generated control signals can be applied experimentally using, for example, a shaker or PZT actuator. To show this issue also in time domain, the impulse responses of the designed controllers are calculated and plotted in Fig. 11 in the same way stated in Section III. Comparison of the magnitude of these impulse responses with the one of the flexible beam in Fig. 7 confirms the applicability of the designed controller for real-time implementation.

VI. Conclusion

Robust control and performance tradeoff in the design of an active vibration control system for a flexible beam is investigated in this brief. The nominal plant of the system is obtained by fitting a continuous transfer function to the measured FRF of the beam. Three modes in the frequency range of 100–400 Hz are selected for control, and the other three modes of the beam are assumed as the uncertainty of the model. Two different weighting functions with loose and tight fitting of uncertainty are selected to show the robustness and performance tradeoffs in the minimax LQG control technique. The aim is to design a controller with good robust stability and performance against model and noise uncertainties. By transforming the minimax LQG control problem to its equivalent H_∞ control problem, the performance and stability robustness of this controller is analyzed and the effect of different design parameters, especially the uncertainty weighting function, is investigated. It is shown that selecting a conservative weighting function for the uncertainty model may lead to robust stability. However, the designer should make a good tradeoff between stability margin and performance of the closed-loop system, and this is mainly achieved by suitably choosing the magnitude of the uncertainty weighting function at different frequencies in the control bandwidth.

References

[1] C. R. Fuller and A. H. von Flotow, "Active control of sound and vibration," *IEEE Control Syst. Mag.*, vol. 15, no. 6, pp. 9–19, Dec. 1995.

[2] A. Preumont, *Vibration Control of Active Structures: An Introduction*. New York: Springer, 2002.

[3] D. C. Hyland, J. L. Junkins, and R. W. Longman, "Active control technology for large space structures," *J. Guid., Control, Dyn.*, vol. 16, no. 5, pp. 801–821, 1993.

[4] C. F. Ross and M. R. J. Purver, "Active cabin noise control," presented at the Active, Budapest, Hungry, 1997.

[5] W. Gawronski, *Advanced Structural Dynamic and Active Control of Structures*. New York: Springer-Verlag, 2004.

[6] R. Marquez and M. Rios-Bolivar, "Active control of vibrations using generalized PI control: An application to a non-linear mechanical system," in *Proc. IEEE Int. Conf. Control Appl. (CCA)*, 2002, pp. 327–332.

[7] J. C. Carmona and V. M. Alvarado, "Active noise control of a duct using robust control theory," *IEEE Trans. Control Syst. Technol.*, vol. 8, no. 6, pp. 930–938, Nov. 2000.

[8] Y.-R. Hu and A. Ng, "Active robust vibration control of flexible structures," *J. Sound Vib.*, vol. 28, pp. 43–56, 2005.

[9] G. Foutsitzi, D. G. Marinova, E. Hadjigeorgiou, and G. E. Stavroulakis, "Robust H_2 vibration control of beams with piezoelectric sensors and actuators," in *Proc. Int. Conf. Phys. Control*, 2003, pp. 157–162.

[10] D. Halim and S. R. Moheimani, "Spatial H_2 control of a piezoelectric laminate beam: Experimental implementation," *IEEE Trans. Control Syst. Technol.*, vol. 10, no. 4, pp. 533–546, Jul. 2002.

[11] D. Halim and S. R. Moheimani, "Experimental implementation of spatial H_∞ control on a piezoelectric laminate beam," *IEEE/ASME Trans. Mechatronics*, vol. 7, no. 3, pp. 346–356, Sep. 2002.

[12] M. Karkoub and K. Tamma, "Modeling and μ-synthesis control of flexible manipulators," *Comput. Structures*, vol. 79, no. 5, pp. 543–551, 2001.

[13] G. J. Balas and J. C. Doyle, "Robustness and performance trade-offs in control design for flexible structures," *IEEE Trans. Control Syst. Technol.*, vol. 2, no. 4, pp. 352–361, Dec. 1994.

[14] F. Paganini and E. Feron, "LMI methods for robust H_2 analysis: A survey with comparisons," *Recent Advances on LMI Methods in Control SIAM*, pp. 129–151, 1999.

[15] I. R. Petersen, V. Ugrinovskii, and A. V. Savkin, *Robust Control Design Using H_∞ Methods*. London, U.K.: Springer-Verlag, 2000.

[16] I. R. Petersen and H. R. Pota, "Minimax LQG optimal control of a flexible beam," *Control Eng. Pract.*, vol. 11, pp. 1–15, Oct. 2002.

[17] J. Hong and D. S. Bernstein, "Bode integral constraints, colocation, and spillover in active noise and vibration control," *IEEE Trans. Control Syst. Technol.*, vol. 6, no. 1, pp. 111–120, Jan. 1998.

[18] I. R. Petersen, M. R. James, and P. Dupuis, "Minimax optimal control of stochastic uncertain systems with relative entropy constraints," *IEEE Trans. Autom. Control*, vol. 45, no. 3, pp. 398–412, Mar. 2000.

[19] T. Inanc, M. Sznaier, P. A. Parrilo, and R. S. Sanchez Pena, "Robust identification with mixed parametric/nonparametric models and time/frequency-domain experiments: Theory and an application," *IEEE Trans. Control Syst. Technol.*, vol. 9, no. 4, pp. 608–617, Jul. 2001.

[20] M. J. Englehart and M. C. Smith, "A four-block problem for H_∞ design: Properties and applications," *Automatica*, vol. 27, no. 5, pp. 811–818, 1991.